

# 2-D NONSEPARABLE WAVELET FILTER BANK WITH ADAPTIVE FILTER PARAMETERS

*Damir Seršić*  
*Miroslav Vrankić*

Department of Electronic Systems and Information Processing  
Faculty of EE & CS, Zagreb HR-10000, CROATIA  
Tel: +385 1 6129940; fax: +385 1 6129652  
e-mail: Miroslav.Vrankic@FER.hr

## ABSTRACT

In this paper, a novel realization of two-dimensional nonseparable wavelet filter bank with adaptive filter parameters is proposed. Two-dimensional generalization of the previously presented 1-D scheme [4] is based on nonseparable quincunx decimation. 2-D filters are designed directly rather than obtained from 1-D filters using the pyramid scheme. Described space variant wavelet filter bank has several advantages when compared to fixed banks. Basic convergence and regularity properties of the limit wavelet functions and scales are provided by fixed part of the filter bank. Variable part of the bank adapts to the analyzed signal. Realization is based on the lifting scheme, derived from a method of fixed 2-D wavelet filter bank design. Original 2-D interpolation of samples in the space domain is modified to an approximation scheme that can be recomputed at each step of decomposition. Adaptation criterion is calculated from wavelet coefficients. Wavelet filter banks with adaptive filter parameters can outperform fixed banks in a number of applications, but the suitable adaptation criterion is still to be found.

## 1 INTRODUCTION

Analytical properties of wavelet filter banks are closely related to the convergence and regularity of limit wavelet functions and scales. More zero moments correspond to higher regularity, which results in better description of smooth and correlated parts of the analyzed image [1]. A number of well-known wavelet families has been developed, based on criteria such as orthogonality, minimum phase, symmetric or near symmetric impulse response, and many others. Number of vanishing moments of a fixed filter bank is usually chosen as a compromise between filter complexity and desired regularity. For a given order, wavelet filters usually have all zeros of their frequency response on Nyquist or DC frequency. But, it does not necessary result in maximum selectivity of the filter bank for a given input image.

Proposed scheme enables changes of filter parameters of both 2-D filters in the bank at each point of decomposition, depending on the local properties of the analyzed image. Two-dimensional nonseparable PR filter bank is intended to form a wavelet tree or wavelet packet tree, so the convergence and some degree of regularity must remain. The adaptation criterion is computed from wavelet coefficients, with the goal of more compact representation of the analyzed signal.

In section 2 we describe construction of the proposed adaptive 2-D filter bank. Kovačević and Sweldens [2] proposed a construction of wavelet families of increasing order in arbitrary dimensions. The

construction is based on the lifting scheme (paragraph 2.1), using interpolation of samples in the multi-dimensional space. Among different nonseparable 2-D polyphase decomposition schemes, we have chosen quincunx decimation (paragraph 2.2). A sketch of the construction is given in paragraph 2.3. Samples from one coset are estimated from the other using 2-D interpolation functions of different orders.

In paragraph 2.3 we explain the proposed structure of the adjustable lifting step. In chapter 3 we discuss the filter bank properties. To ensure convergence and minimum regularity, filters are split in the fixed and variable part. Filter parameters can be changed at each point of decomposition, as well as the associated limit wavelet functions and scales. We deal with a kind of second generation 2-D wavelets. Fixed vanishing moments plus limitations on variable filter parameters ensure convergence and reasonable regularity of decomposition functions.

## 2 FILTER BANK STRUCTURE

### 2.1 Lifting scheme

The lifting scheme enables easy construction of perfect reconstruction time or space variant and non-linear filter banks. Daubechies and Sweldens 98 [3] show that any two-band FIR filter bank can be factored in a set of lifting steps, using Euclidean algorithm.

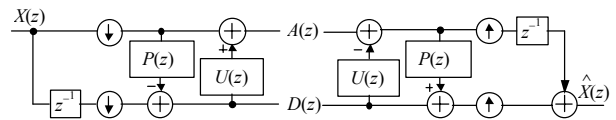


**Figure 1.** One-dimensional 2-channel PR filter bank factored in lifting and dual lifting steps.

The polyphase matrix of the filter bank from **Figure 1** is factored in two triangular sub-matrices:

$$\mathbf{P}(z) = \begin{bmatrix} 1 & 0 \\ U(z) & 1 \end{bmatrix} \cdot \begin{bmatrix} 1 & -P(z) \\ 0 & 1 \end{bmatrix},$$

$$H(z) = z^{-1} - 1 \cdot P(z^2),$$

$$L(z) = 1 + H(z) \cdot U(z^2).$$

### 2.2 Lifting scheme in two dimensions with quincunx decimation

A straightforward way of implementing 2-D lifting scheme is generalization of 1-D scheme in two dimensions that is called

Mallat pyramid scheme.

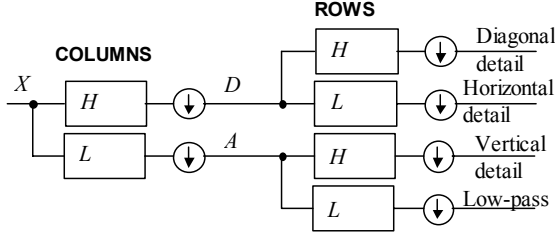


**Figure 2.** Two-dimensional sub-band decomposition using separable pyramid algorithm.

It can be seen from **Figure 2** that this approach is separable, treating differently columns and rows. Because of its horizontal and vertical bias it cannot be considered as a truly two-dimensional approach. This bias will introduce perceptually greater distortion after applying nonlinear operations on wavelet coefficients (such as soft thresholding and quantization). Truly two-dimensional transforms that treat all directions in the picture similarly are better tuned to the human visual system and therefore preferred.

We used nonseparable quincunx decimation. Quincunx decimation decomposes the input image into two cosets as shown in the right of **Figure 3**.

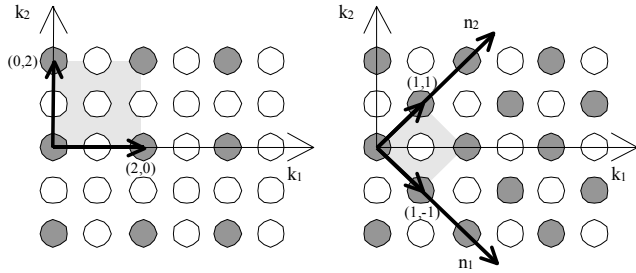


**Figure 3.** Separable (left) and quincunx nonseparable lattice (right) with their unit cells (marked gray).

Subsampling matrix  $\mathbf{D}$  for quincunx decimation is defined through a pair of vectors that form quincunx unit cell:

$$\mathbf{D} = \begin{bmatrix} 1 & 1 \\ -1 & 1 \end{bmatrix}, \quad \begin{bmatrix} k_1 \\ k_2 \end{bmatrix} = \mathbf{D} \cdot \begin{bmatrix} n_1 \\ n_2 \end{bmatrix}.$$

Hence, proposed 2-D filter bank block scheme is almost the same as the one shown in **Figure 1**. 1-D polyphase decomposition is replaced by the 2-D nonseparable quincunx decimation scheme and the 1-D interpolating prediction and update filters are changed to their 2-D equivalents.

### 2.3 Adjustable lifting step

We construct the prediction filter as a weighted sum of additive components:

$$P(z_1, z_2) = p_1 \cdot P_2(z_1, z_2) + p_2 \cdot [P_4(z_1, z_2) - P_2(z_1, z_2)] + p_3 \cdot [P_6(z_1, z_2) - P_4(z_1, z_2)] + p_4 \cdot [P_8(z_1, z_2) - P_6(z_1, z_2)] + \dots$$

Filters  $P_2, P_4, P_6$  and  $P_8$  are Neville interpolating filters that are constructed as described in Kovačević and Sweldens [2]. Symmetric interpolation neighborhoods (rings shown in **Figure 5**) are selected and de Boor-Ron algorithm is used to construct  $P_2, P_4, P_6$  and  $P_8$  filter coefficients. The coefficients are given in **Table 1**. Higher filter orders require more neighboring rings to be involved.

If the multiplying parameters  $\{p_1, p_2, p_3, p_4\}$  are constant, chosen from sets  $\{1, 0, 0, 0\}_I, \{1, 1, 0, 0\}_{II}, \{1, 1, 1, 0\}_{III}$  and  $\{1, 1, 1, 1\}_{IV}$ , lifting

steps  $P_2(z_1, z_2), P_4(z_1, z_2), P_6(z_1, z_2)$  and  $P_8(z_1, z_2)$  respectively are obtained. They correspond to 2, 4, 6 or 8 zero moments of the associated 2-D wavelet function.

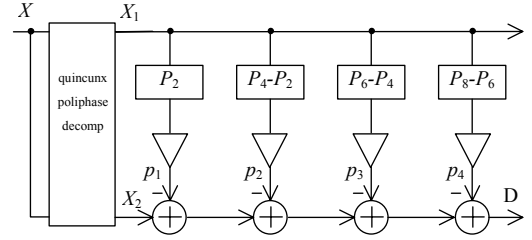


**Figure 4.** Structure of the proposed adaptive lifting step (prediction stage).  $P_2, P_4, P_6$  and  $P_8$  are Neville 2-D interpolating filters,  $p_2, p_4, p_6$  and  $p_8$  are variable parameters.

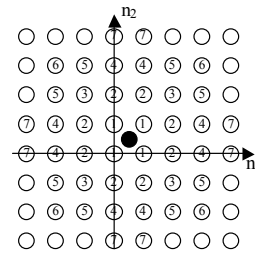


**Figure 5.** Quincunx lattice in the sampled domain containing  $X_1$  coset samples. Ring numbers are marked. Black circle represents position of the predicted sample in coset  $X_2$ .

$N$	ring 1	ring 2	ring 3	ring 4	ring 5	ring 6	ring 7	
2	1							$\times 2^{-2}$
4	10	-1						$\times 2^{-5}$
6	174	-27	2	3				$\times 2^{-9}$
8	23300	-4470	625	850	-75	9	-80	$\times 2^{-16}$

**Table 1.** Quincunx Neville filters coefficients.  $N$  is the number of vanishing moments.

An example constructed using **Figure 5** and **Table 1**:

$$P_4(z_1, z_2) = (10 + 10z_1^{-1} + 10z_2^{-1} + 10z_1^{-1}z_2^{-1} - z_1^{-2} - z_2^{-2} - z_1^{-2}z_2^{-1} - z_1^{-1}z_2^{-2} - z_1 - z_2 - z_1z_2^{-1} - z_1^{-1}z_2) / 32.$$

Structure in **Figure 4** enables splitting of prediction filter in the fixed and variable part. Desired number of vanishing moments is achieved by fixing factors  $p_1$  to  $p_4$ . For example,  $p_1=1$  results in 2, or  $p_1=p_2=1$  results in 4 vanishing moments. Residual parameters are used as variables that can be changed at each point of decomposition.

### 2.4 Adjustable dual lifting step

Construction of the adaptive update step is shown in **Figure 6**. Now, let us fix multiplying factors  $\{p_1, p_2, p_3, p_4\}$  to ones and zeros according to sets I-IV from the previous paragraph. Each set results in one of the corresponding well known  $P_2, P_4, P_6$  and  $P_8$  predictors.

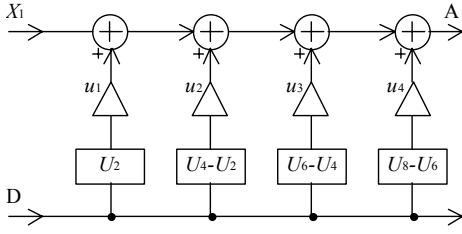


**Figure 6.** Realization of the dual lifting step (update stage)

In order to provide vanishing moments to the limit scale function, we set the gains  $u_i$ :

$p_1, \dots, p_i = 1$	$i=1$ (I)	$i=2$ (II)	$i=3$ (III)	$i=4$ (IV)
$u_1$	1	1	1	1
$u_2$	3/2	1	1	1
$u_3$	–	3/2	1	1
$u_4$	–	3/2	3/2	1

**Table 2.** Gain  $u_i$  depends on the actual number of zeros of the high-pass filter, unless we fix less or equal number of zeros of the low-pass filter.

**Table 2** shows that if the number of zeros of the LP filter ( $f=Nyquist$ ) is less or equal to the number of zeros of the HP filter ( $f=0$ ), gains  $u_i$  equal 1 for all  $i=1-4$ . Thus if the number of fixed gains  $u_i$  does not exceed the number of fixed gains  $p_i$  we have “independent” vanishing moments. Moreover, they do not depend on the remaining free parameters! If we need more zeros for the LP filter, we can simply swap the positions of HP and LP filter by reversing signs of all parameters  $p$  and  $u$ .

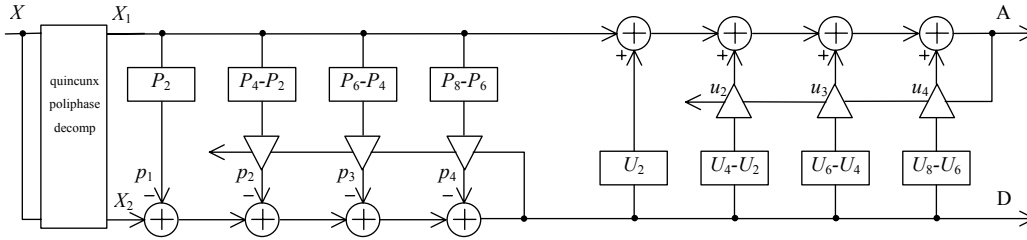


**Figure 7.** Adaptive wavelet filter bank (analysis part) with 2+2 fixed vanishing moments and 3+3 free parameters.

### 3 ADAPTATION CRITERION AND RESULTS

#### 3.1 Tuning of the filter properties

In this section we discuss a realization with 2 vanishing moments fixed on both P and U side and only one free predictor parameter. In other words:  $p_1 = u_1 = 1$  and  $p_2$  is being modified. For the simplicity, all other coefficients are set to zero. Corresponding high pass frequency responses for  $p_1 = u_1 = 1$  and  $p_2 = \{-10, -1, 0, 1, 2, 10\}$  are shown in **Figure 8**.

With  $p_1 = 1$  and  $p_2 = 0$  we obtain linear 2-D interpolating predictor  $P_2$ . Corresponding high pass filter  $H(z_1, z_2)$  has two vanishing moments at  $z_1 = z_2 = 1$ . With  $p_2 = 1$  four vanishing moments are obtained, making transfer function  $H(z_1, z_2)$  more flat around  $z_1 = z_2 = 1$ .

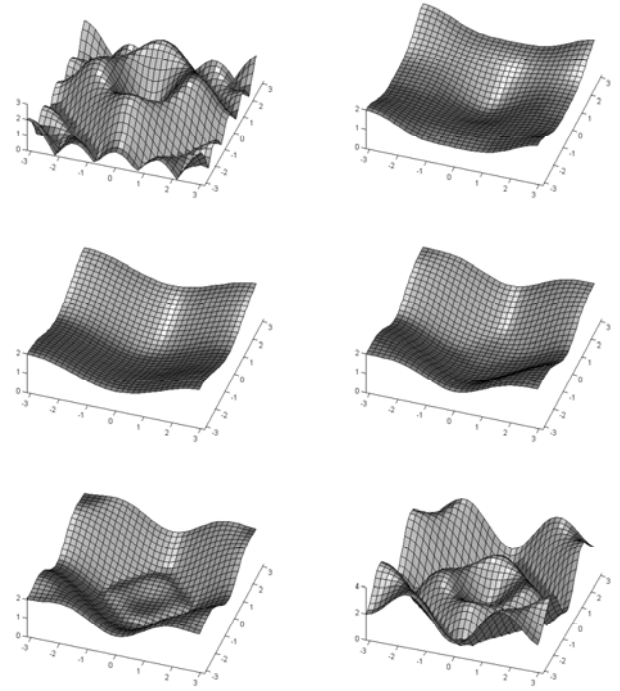


**Figure 8.** Frequency responses of the adaptive two-dimensional HP filter for different values of parameter  $p_2$ . From left to right, top to bottom:  $p_2 = \{-10, -1, 0, 1, 2, 10\}$ . Middle row ( $p_2=0, 1$ ) corresponds to fixed wavelets with 2 and 4 vanishing moments. Parameter values outside  $[0, 1]$  interval cause additional zeros of the response forming nearly rectangular “ditches”.

If parameter  $p_2 > 1$  high pass filter frequency response

$$\left| H(e^{j\omega_1}, e^{j\omega_2}) \right|$$

introduces new zeros outside the origin: a surrounding “ditch” that widens for larger  $p_2$  into a diamond shape up to the limit  $|\omega_1 \pm \omega_2| = \pi$  (see:

bottom of **Figure 9**). If parameter  $p_2$  is set to large negative values, frequency response begins to have zero “ditches” on the opposite side: near high frequency corners (see **Figure 8** and **Figure 9**). High pass filter turns to a kind of band pass, and a problem with convergence appears (**Figure 10**).

Positive values of  $p_1$  are good candidates for achieving desired HP frequency response: zeros on the lower part of the frequency plane can be adjusted to cancel large low-frequency components of the analyzed signal. But, large positive or negative values widen the energetic frame bounds of the transform, thus making filter bank very far from unitary. Moreover, limit functions do not necessarily converge. In practice, the region of acceptable parameter values is bounded. Limit wavelet functions for several values of parameter  $p_1$  are shown in **Figure 10**.

We applied the adaptive wavelet filter bank to a synthetic image  $X$  composed of 2 horizontal sine waves of different frequencies. If we set  $p_2$  to two appropriate values in areas corresponding to different sine frequencies, decomposition is near optimal. Almost everywhere wavelet coefficients are turned to zero (**Figure 11**).

The question is: Is there a method to find appropriate filter parameters automatically? The complete answer is left for future research.

We used a one-dimensional RLS adaptation algorithm, using a “snake-like” collection of pixels for 2-D to 1-D mapping (**Figure 11**). The adaptation criterion follows the frequency of the analyzed signal, trying to turn detail coefficients to zero after the adaptation. Wavelet functions change at each step of decomposition, somewhere “in between” of those shown in **Figure 10**, so the good regularity properties remain.

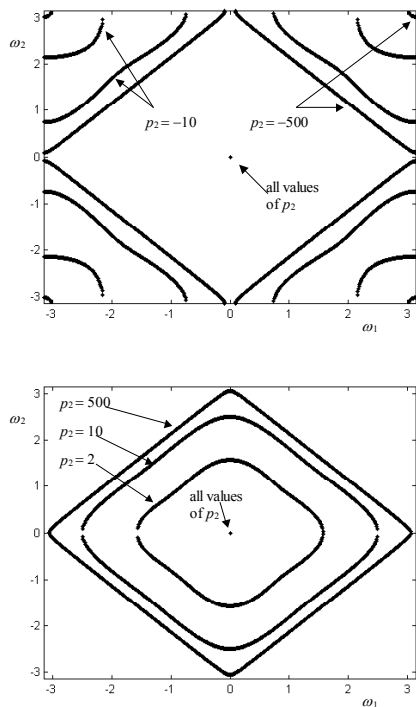


**Figure 9.** Zero locations in frequency responses of the adaptive two-dimensional HP filter for different values of parameter  $p_2$ . Top: negative values of  $p_2$ . Bottom: positive values of  $p_2$ .

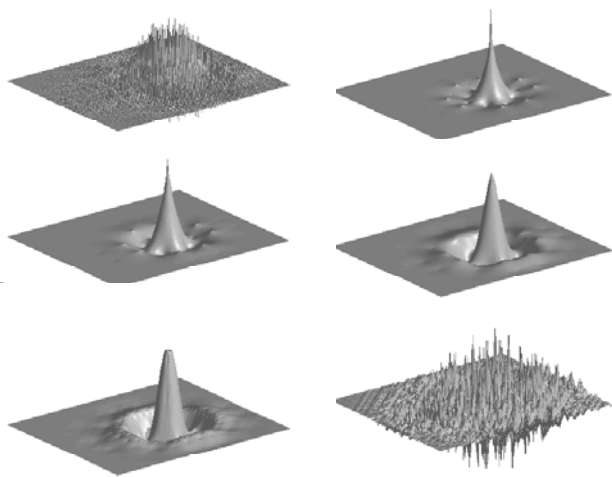


**Figure 10.** Limit wavelet functions for different values of parameter  $p_2$ . From left to right, top to bottom:  $p_2 = \{-10, -1, 0, 1, 2, 10\}$ . Large parameter values such as  $|p_2|=10$  cause divergence.

In general, we can reconstruct the analyzed image from wavelet coefficients plus information on filter parameters  $\{p_{mn}\}$  and  $\{u_{kl}\}$ . They are expected to be coded very efficiently. For 1-D adaptive wavelets [4] strictly causal adaptation criterions could be self-reproduced on the reconstruction side, with no need for filter parameters to be separately transferred. Whenever one-dimensional adaptation algorithm is used the causality criterion for self-reproduction still holds. Of course, such adaptation algorithm is far from optimal when applied to 2-D images.

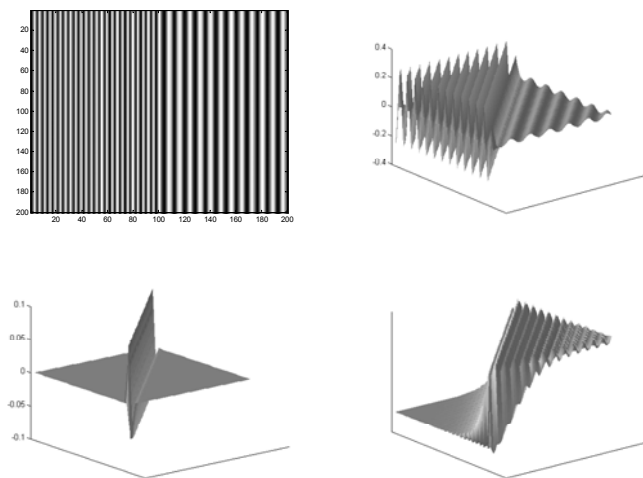


**Figure 11.** Top left: analyzed image  $X$  composed from 2 horizontal sine waves ( $\omega_1 = \pi/2, \pi/4$ ). Top right: wavelet coefficients  $D$  for fixed predictor  $P_4$  (only central part is shown). Bottom left: wavelet coefficients  $D$  for adapted predictor:  $p_2$  has values 2 and 1.17. Bottom right:  $p_2$  as a result of 1-D adaptive RLS algorithm ( $\lambda = 0.85$ ).

## 4 Conclusion

We give a novel realization of the two-dimensional nonseparable adaptive wavelet filter bank. Prediction and update filters are implemented as a ladder of filter sections, where each successive section brings the contribution of the higher order approximation. A set of filter parameters is fixed and determines the desired number of zero moments. Free parameters can change at each point of decomposition or reconstruction. We used the recursive least square error criterion, computed from wavelet coefficients. Adaptive filter bank is applied on a synthetic signal. Wavelet coefficients get close to what we expect to be an optimal representation of the analyzed signal. Described 2-D space variant wavelet filter bank is more suitable for analysis of non-stationary images than fixed banks. Proper choice of the adaptation algorithm is still a problem for future research.

## References

- [1] Daubechies I., Orthonormal Bases of Compactly Supported Wavelets, *Comm. on Pure and Appl. Math.*, 41:909-996, 1988
- [2] Kovačević J. and Sweldens W., Wavelet Families of Increasing Order in Arbitrary Dimensions, *IEEE Trans. on Image Proc.*, 9(3):480-496, 2000
- [3] Daubechies I. and Sweldens W., Factoring Wavelet Transforms into Lifting Steps, *J. Fourier Anal. and Appl.*, 4(3):247-269, 1998
- [4] D. Seršić, A Realization of Wavelet Filter Bank with Adaptive Filter Parameters, *Proc. of EUSIPCO 2000*, 3:1733-1736, 2000